VOL. 17, NO. 4, APRIL 1980 J. AIRCRAFT
ARTICLE NO. 80-4028

C80-036

Prandtl's Biplane Theory Applied to Canard and Tandem Aircraft

00006
00024

E. V. Laitone*
University of California, Berkeley, Calif.

Prandtl's biplane theory for elliptic loadings is generalized to apply to nonelliptic spanwise load distributions. The induced drag is calculated by assuming an infinite stagger distance so all of the mutually induced drag acts upon the rear surface which has no effect upon the front surface. Consequently, the mutually induced drag is calculated by integrating the Trefftz-plane downwash of the front surface over the independent load distribution on the rear surface. This procedure is verified by explicit solutions that give the same mutually induced drag irrespective of the fore and aft location of the larger span when carrying either an elliptic or a uniform load distribution. It was found that the mutually induced drag was less when the larger span had a uniform load distribution, but the total induced drag was not decreased because of the additional self-induced drag produced by the change from the ideal elliptic loading to a uniform loading. However, when the larger span carried a uniform loading it allowed the smaller span, when either fore or aft, to support more of the aircraft's weight at the minimum induced drag condition.

Nomenclature

A	= aspect ratio of lifting surface
b	= span of lifting surface
C_{D_i}	= induced drag coefficient, D_i/qS
C_L	= lift coefficient, L/qS
D_i	= total induced drag force
D_m	= minimum total induced drag force
D_0	= referenced induced drag when $b_2 > b_1$, $(W^2/\pi q b_2^2)$, Eq. (14)
$1/e$	= increase of self-induced drag with a nonelliptic load distribution
e_3	= effect of nonelliptic load distribution, or roll up of the trailing vortex sheet, on the Trefftz-plane downwash of front surface (*1*)
g	= gap or vertical separation distance
L	= lifting force
q	= dynamic pressure, $\rho V^2/2$
S	= planform area of lifting surface
V	= freestream or flight velocity
W	= total weight of aircraft, $L_1 + L_2$
$w_1(\infty,y,g)$	= downwash velocity component produced by (*1*) in its Trefftz-plane
w_0/V	= downwash angle produced by (*1*) in the center of its Trefftz-plane, $(2C_{L_1}/\pi A_1)$ when its spanwise load distribution is elliptic
σ	= Prandtl's mutually induced drag factor, Eq. (2)

Subscripts

(0)	= corresponding to $L_0 = W$, Eq. (13)
(1)	= front lifting surface
(2)	= rear lifting surface

I. Introduction

PRANDTL'S[1] biplane theory was applied by Laitone[2] to evaluate the induced drag of wing-tail combinations that were not coplanar. It was shown that a finite gap, or vertical separation distance, led to a small positive tail load for minimum induced drag. This analysis will now be extended to typical canard and tandem aircraft configurations which have nonelliptic, as well as the usual ideal elliptic, spanwise load distributions on either one of the lifting surfaces. The calculations for Prandtl's σ factor that determines the mutually induced drag were carried out in Refs. 1 and 2 only for the special case when both lifting surfaces carried the ideal elliptic load distribution. The present analysis extends these results to include the cases when either, or both lifting surfaces have a uniform load distribution.

Prandtl[1] calculated the mutually induced drag factor σ by proving that the contribution of the bound vortex systems of both lifting surfaces cancelled each other exactly so the total induced drag could be calculated by considering only the effect of each trailing vortex system for the case of zero stagger distance. Later Laitone[2] showed that it was advantageous to consider the limiting case of an infinite stagger distance so that all of the mutually induced drag would act upon the rear surface (*2*) *which would have no influence upon the front surface* (*1*). Consequently, the total mutually induced drag between two interacting lifting surfaces could be calculated most easily by simply integrating the effect of the Trefftz-plane downwash of (*1*) upon the independent load distribution of (*2*). One purpose of the present paper was to confirm the validity of this procedure for various load distributions by showing that the mutually induced drag so calculated was independent of the fore and aft configuration, that is independent of whether the larger span was either ahead of or behind the smaller span as long as the lift distributions on each lifting surface remained the same and the gap or vertical separation distance was the same. These results satisfied Munk's stagger theorem (e.g., see Ref. 3, pp. 131-133) which proved that the total induced drag was independent of any translation (fore or aft) in the flight direction as long as the circulation distributions remained the same. It is also shown that as in the case of the elliptic load distributions, the mutually induced drag for uniform load distributions is the same if the larger span is either above or below the smaller span, as long as the gap is the same. These statements were confirmed by explicit solutions for both elliptic and uniform load distributions that were valid for any span ratios. It was found that when the larger span, either fore or aft, had a uniform lift distribution then the total mutually induced drag was less than that produced when the larger span had the ideal elliptic load distribution. However, as would be expected, this decrease in the mutually induced drag when the larger span carried a uniform load was offset by the increase in the self-induced drag produced by the

Received April 13, 1979; revision received Oct. 29, 1979.

Index categories: Performance; Configuration Design.

*Professor, Department of Mechanical Engineering. Associate Fellow AIAA.

uniform load itself. That is, the larger span had its induced drag increased by the departure from the ideal elliptic load distribution; consequently, the total induced drag was not decreased even though the mutually induced drag had been decreased. Finally, it is indicated how the mutually induced drag of a canard or tandem aircraft could be decreased by having the larger span rear surface carry a load distribution similar to that produced by a constant chord wing. Although the total induced drag was increased, this modification of the larger span's elliptic load distribution allowed the smaller span front surface to carry a larger fraction of the aircraft weight at the minimum induced drag condition.

II. Mutually Induced Drag when $L_1(y_1)$ is Elliptic

Laitone[2] showed that Prandtl's[1] potential flow relation for the total induced drag created by two interacting lifting surfaces with elliptic load distributions could be modified for nonelliptic load distributions and real viscous flow effects by introducing the nondimensional coefficients based on $S=S_1>S_2$, as given in the Nomenclature,

$$C_{D_i}=\frac{C_{L_1}^2}{\pi A_1 e_1}+\frac{\sigma}{e_3}\frac{b_1}{b_2}\frac{2C_{L_1}}{\pi A_1}\frac{S_2}{S_1}C_{L_2}+\frac{S_2}{S_1}\frac{C_{L_2}^2}{\pi A_2 e_2}=\frac{D_i}{qS_1} \tag{1}$$

where $e_1<1$ and $e_2<1$ represent any departure from the ideal elliptic load distributions with $e_1=1=e_2$ as assumed in Prandtl's relation, while the correction factor $e_3>1$ represents any departure from the ideal Trefftz-plane downwash corresponding to an elliptic load distribution on the front surface (*1*). For example, the inviscid rollup of the trailing vortex sheet of the front lifting suface (*1*) would correspond to $e_3\approx 1.23$ for a coplanar rear lifting surface (*2*) having a much smaller span. Prandtl[1] only considered the ideal potential flow downwash produced by an elliptic load distribution so that $e_3=1$ while the factor $\sigma b_1/b_2$ gave the decrease in the Trefftz-plane downwash as the vertical separation or gap distance g increases. We can now generalize Prandtl's σ factor for the mutually induced drag by writing

$$\frac{\sigma}{e_3}\frac{b_1}{b_2}=\frac{1}{L_2}\int_{-b_2/2}^{b_2/2}\frac{w_1(\infty,y_2,g)}{w_0}\mathrm{d}L_2(y_2) \tag{2}$$

where $w_o/V=2C_{L_1}/\pi A_1$. This generalized relation reduces to Eq. (14) of Ref. 2 when $e_3=1$ and it will be shown how it can be used to determine σ/e_3 for any $L_1(y_1)$ or $L_2(y_2)$ load distributions.

If the front lifting surface (*1*) has the ideal elliptic load distribution then its Trefftz-plane downwash is given by (e.g., see Ref. 3, p. 148)

$$[w_1(\infty,y,g)/w_0]=R_e\{1-(y+ig)[(y+ig)^2-(b_1/2)^2]^{-\frac{1}{2}}\} \tag{3}$$

For zero gap this downwash reduces to

$$\frac{w_1(\infty,y,0)}{w_0}=\begin{cases}1 & \text{for } |y|\le b_1/2\\ 1-(2y/b_1)[2y/b_1)^2-1]^{-\frac{1}{2}} & \text{for } |y|>b_1/2\end{cases} \tag{4}$$

Equations (2) and (4) show immediately that when the gap is zero then $\sigma/e_3=\sigma=b_2/b_1\le 1$ for any load distribution upon a smaller span rear lifting surface (*2*). However, if the rear lifting surface has a larger span than the front lifting surface, corresponding to a canard or tandem-type aircraft, then this simple result applies in the form $\sigma/e_3=\sigma=b_1/b_2\le 1$ only if $L_2(y_2)$ is also elliptic so that Eq. (1) can be written as (e.g., see Ref. 3, p. 217)

$$\frac{\sigma}{e_3}\frac{b_1}{b_2}=\frac{4}{\pi}\int_0^1\frac{w_1(\infty,y_2,g)}{w_0}[1-(2y_2/b_2)^2]^{\frac{1}{2}}\mathrm{d}(2y_2/b_2) \tag{5}$$

After substituting Eq. (4) for zero gap into Eq. (5) we obtain, as before for $b_2\le b_1$, $\sigma/e_3=b_2/b_1\le 1$; similarly, when $b_2\ge b_1$ we obtain the equivalent relation $\sigma/e_3=b_1/b_2\le 1$. However, when $L_2(y_2)$ is constant, corresponding to a uniform lift distribution, then when $b_2>b_1$ we obtain from Eqs. (2) and (4) for zero gap

$$\frac{\sigma}{e_3}\frac{b_1}{b_2}=\frac{2}{b_2}\left[\int_0^{b_2/2}\mathrm{d}y_2-\int_{b_1/2}^{b_2/2}(2y_2/b_1)[(2y_2/b_1)^2-1]^{-\frac{1}{2}}\mathrm{d}y_2\right]=1-[1-(b_1/b_2)^2]^{\frac{1}{2}}<1 \tag{6}$$

Since $b_1/b_2<1$ we can expand this relation to the following infinite series,

$$\frac{\sigma}{e_3}=\left[\frac{1}{2}\left(\frac{b_1}{b_2}\right)+\frac{1}{8}\left(\frac{b_1}{b_2}\right)^3+\frac{1}{16}\left(\frac{b_1}{b_2}\right)^5+\frac{5}{128}\left(\frac{b_1}{b_2}\right)^7+\ldots\right]<1 \tag{7}$$

which converges only for $b_1/b_2<1$. Note that $e_3\to 2$ for $b_2\gg b_1$ since $\sigma/e_3\to\frac{1}{2}(b_1/b_2)$, as may be seen in Fig. 1. As shown by the dotted line in Fig. 1, Eq. (6) predicts a considerably smaller mutually induced drag than that corresponding to the elliptic L_2 distribution, which is also given in Fig. 1 by $\sigma/e_3=\sigma=b_1/b_2<1$ for the zero gap case. However, as will be shown, the induced drag of the larger span ($b_2>b_1$) rear lifting surface is increased by $e_2<1$, since it has a uniform rather than an ideal elliptic load distribution with $e_2=1$; consequently, the total induced drag is not decreased even though the mutually induced drag has been decreased. The dotted lines representing the uniform L_2 in Fig. 2 are calculated for $e_2=1$, so the actual value of $e_2<1$ would raise D_m/D_0 above solid lines.

The σ/e_3 values were numerically calculated for several constant gap ratios by substituting the numerical values from Eq. (3) into Eq. (5), corresponding to an ideal elliptic load distribution on both surfaces so $e_3=1$. Incidentally, these numerical calculations are considerably simplified by using Eq. (3) rather than the equivalent expression given on pages 149 and 217 (Eq. 22.6) of Ref. 3 since the latter is very difficult to evaluate for a constant gap ratio. The numerically calculated values in Fig. 1 are in accord with Munk's stagger theorem since the σ/e_3 values are the same when the values of $b_2/b_1<1$ correspond to the values of $b_1/b_2<1$. That is the σ/e_3 values for the solid lines with $e_3=1$ (since both surfaces have the ideal elliptic loading) are the same whether the larger surface is fore or aft as long as the constant gap ratio is always based upon the larger span, as shown in Fig. 1. For the special case of zero gap, we can explicitly verify Munk's stagger theorem from Eqs. (2, 4, and 5). For example when $L_1(y_1)$ and $L_2(y_2)$ are both elliptic load distributions then $e_3=1$ and σ is either given by $b_2/b_1\le 1$, or by $b_1/b_2\le 1$, for the zero gap or coplanar case. Then for $b_2>b_1$, again for zero gap, Eq. (7) shows that in the limiting case of a large span b_2 uniform load distribution aft of a small span b_1 elliptic load distribution we have $\sigma/e_3=\frac{1}{2}(b_1/b_2)$. This same limiting case occurs, in the form $\sigma/e_3=\frac{1}{2}(b_2/b_1)$, if the larger span b_1 uniform load distribution is placed ahead of the smaller span b_2 elliptic load distribution, since the Trefftz-plane downwash behind the centerline of a uniform load distribution is given by $w_1/V=C_{L_1}/\pi A_1$, exactly one-half of the corresponding value for an elliptic load distribution; consequently, Eq. (2) gives a limiting value of $\sigma/e_3=\frac{1}{2}(b_2/b_1)$ as $b_2\to 0$. In the

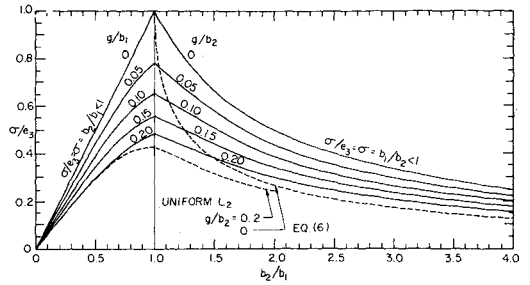

Fig. 1 Variation of σ/e_3 with span ratio for constant gap ratio, when L_1 elliptic and L_2 either elliptic ($e_3=1$, solid line) or uniform ($e_3>1$, dotted line).

next section it will be shown that σ is independent of the fore and aft location of the larger span with the uniform load distribution for all span ratios.

III. Mutually Induced Drag when $L_1(y_1)$ is Constant

When the front lifting surface (*1*) has a uniform load distribution, then its downwash in the Trefftz-plane is given by (e.g., see Ref. 3, p. 218)

$$\frac{w_1(\infty,y,g)/V}{(2C_{L_1}/\pi A_1)}=\frac{1}{4}\left[\frac{(1+2y/b_1)}{(1+2y/b_1)^2+(2g/b_1)^2}+\frac{(1-2y/b_1)}{(1-2y/b_1)^2+(2g/b_1)^2}\right] \tag{8}$$

As previously noted, $w_1(\infty,0,0)/V=C_{L_1}/\pi A_1$, which is exactly one-half the corresponding downwash produced by the elliptic load distribution in Eq. (4).

If we now consider the case of zero gap and introduce Eq. (8) for $L_1(y_1)$ uniform into Eq. (5) for $L_2(y_2)$ elliptic, we obtain

$$\frac{\sigma}{e_3}\frac{b_1}{b_2}=\frac{1}{\pi}\int_0^1\left[\frac{1}{1+2y_2/b_1}+\frac{1}{1-2y_2/b_1}\right]\times[1-(2y_2/b_2)^2]^{-1/2}\,\mathrm{d}(2y_2/b_2)$$

$$=\left(\frac{b_1}{b_2}\right)^2\left\{1-\left[1-\left(\frac{b_2}{b_1}\right)^2\right]^{1/2}\right\}\quad\text{for } b_1\geq b_2 \tag{9}$$

which is in exact agreement with Eq. (6), after we interchange b_1 and b_2 to indicate that now the larger span b_1 with the uniform load distribution has become the front surface ahead of the rear smaller span b_2 with the elliptic load distribution. This again is in agreement with Munk's stagger theorem, and in addition, since Eqs. (6) and (9) give identical explicit relations, this verifies the use of Eq. (2) to calculate the mutually induced drag of two interacting lifting surfaces. In other words, as first pointed out in Ref. 4, the total mutually induced drag can be calculated by assuming that the rear surface is an infinite distance behind the front surface so it cannot induce any drag on the front surface. Sachs[5] indicates that he has independently verified this conclusion for noncoplanar lifting surfaces.

It should be noted that Eq. (6), and not Eq. (9), has been shown in Fig. 1 which only illustrates the variation of σ/e_3 as the front lifting surface distribution remains elliptic while the rear load distribution changes from elliptic (solid line) to uniform (dotted line). Consequently, the dotted line σ/e_3 values are not the same when the span ratio is the same since the uniform load distribution remains on the rear surface (*2*) whether or not it is either the smaller span when $b_2/b_1<1$, or the larger span when $b_2/b_1>1$. In this case, Munk's stagger theorem is not satisfied as it is by Eqs. (6) and (9) which represent a uniform load distribution on the larger span, and an elliptic load distribution on the smaller span, irrespective of their fore and aft configurations. The dotted line for zero gap in Fig. 1 coincides with the solid line for $\sigma/e_3=b_2/b_1\leq 1$ since the larger front surface has the elliptic load distribution that produces the constant Trefftz-plane downwash described by Eq. (4); consequently, as previously discussed, any load distribution on the smaller span rear surface that is coplanar would reduce Eq. (2) to $\sigma/e_3=\sigma=b_2/b_1\leq 1$.

An explicit relation for the mutually induced drag for a small span tail at any distance above or below a large span wing with an elliptic load distribution was given by Laitone,[2] and it is confirmed by Eqs. (2) and (3) which show that in the limiting case of a small span tail with any load distribution we have

$$\frac{\sigma}{e_3}\frac{b_1}{b_2}=\frac{w_1(\infty,0,g)}{w_0}=1-\frac{2g}{b_1}\left[1+\left(\frac{2g}{b_1}\right)^2\right]^{-1/2} \tag{10}$$

as long as the wing has an elliptic load distribution that produces the Trefftz-plane downwash described by Eq. (3). However, if the wing has a uniform load distribution with the Trefftz-plane downwash given by Eq. (8) we obtain

$$\frac{\sigma}{e_3}\frac{b_1}{b_2}=\frac{w_1(\infty,0,g)}{w_0}=\tfrac{1}{2}\left[1+\left(\frac{2g}{b_1}\right)^2\right]^{-1} \tag{11}$$

It is obvious that for the coplanar case with zero gap a very small span tail behind a wing with an elliptic lift distribution has $e_3=1$, since $\sigma/e_3=b_2/b_1$ from Eq. (10); while from Eq. (11) we have $e_3=2$ for a very small span tail behind a wing with a uniform load distribution. However, if the trailing vortex sheet rolls up to produce two vortex cores with a span distance of $\pi b_1/4$ (e.g., see Ref. 3, p. 326), then we have $e_3=\pi^2/8=1.23$ for either the uniform or the elliptic spanwise load distributions, when the gap is zero.

When both load distributions are uniform then Eqs. (2) and (8) integrate to give

$$\frac{\sigma}{e_3}\frac{b_1}{b_2}=\frac{1}{8}\frac{b_1}{b_2}\ln\left[\frac{(1+b_2/b_1)^2+(2g/b_1)^2}{(1-b_2/b_1)^2+(2g/b_1)^2}\right] \tag{12}$$

For any finite gap Eq. (12) applies to all span ratios, and for zero gap we also obtain this result if $b_2<b_1$. However, when $b_2\geq b_1$, we find that Eq. (2) can only be evaluated by taking its Cauchy principle value, and the result corresponds to Eq. (12) with $g=0$ only when $b_2>b_1$. When $b_2=b_1$ we find that σ has no limit for $g=0$; consequently, the mutually induced drag is not defined for coplanar lifting surfaces that have the same span and a uniform load distribution. Equation (12) is in accord with Munk's stagger theorem since the value of σ is independent of the fore and aft configuration. It should also be noted that σ is the same when the larger span is either above or below the smaller span. Since the lift distributions are not elliptic, $e_3>1$; e.g., when the spans are equal ($b_2=b_1$) and the gap ratio is one-fifth the span we have from Eq. (12) $\sigma/e_3=0.4073$, or $e_3=1.189$ as compared to $\sigma/e_3=0.4843=\sigma$ when both load distributions are elliptic as in Fig. 1 (solid line for $g/b_1=0.2=g/b_2$). Similarly, for the dotted line in Fig. 1, corresponding to L_1 elliptic and L_2 uniform, when $b_2=b_1$ we obtain $\sigma/e_3=0.4274$ or $e_3=1.133$ from the numerical evaluation of Eqs. (2) and (3) when $g/b_1=0.2=g/b_2$.

IV. Minimum Total Induced Drag

For the typical noncoplanar wing-tail combination with a tail span b_2 less than the wing span b_1 Laitone[2] showed that the minimum total induced drag (C_{D_m} in Eq. 19 of Ref. 2) occurred with a very small positive tail load (L_2/W in Eq. 18 of Ref. 2). For the case of a canard or tandem-type aircraft having the larger lifting surface span b_2 at the rear so that $b_1/b_2<1$ we can obtain similar results by defining the total

lift coefficient in terms of the larger surface so that $S=S_2>S_1$

$$C_{L_0}=C_{L_2}+(S_1/S_2)C_{L_1}=(W/qS_2) \tag{13}$$

with a reference induced drag defined as

$$D_0=(C_{L_0}{}^2/\pi A_2)qS_2=W^2/\pi qb_2^2 \tag{14}$$

By substituting Eq. (13) into the equivalent form of Eq. (1) based on $D_i=C_{D_i}qS_2$ so as to eliminate C_{L_2} we obtain an expression for the total induced drag C_{D_i} as a function of the smaller lifting surface lift coefficient C_{L_1}. This expression may then be differentiated with respect to C_{L_1} to obtain the following expression for the values of C_{L_1} that gives the minimum C_{D_i} for a given ratio of $b_2/b_1>1$

$$\frac{S_1}{S_2}\frac{C_{L_1}}{C_{L_0}}=\left(1-\frac{\sigma b_2 e_2}{e_3 b_1}\right)\left(1-\frac{2\sigma b_2 e_2}{e_3 b_1}+\frac{b_2^2 e_2}{b_1^2 e_1}\right)^{-1}=\frac{L_1}{W} \tag{15}$$

Therefore, the minimum $C_{D_i}=C_{D_m}$ is given by this value of C_{L_1} for the given span ratio as

$$\frac{C_{D_m}}{C_{L_0}{}^2/\pi A_2}=\left(\frac{1}{e_2}-\frac{\sigma^2 e_1}{e_3^2}\right)\left[1-\frac{2\sigma b_1 e_1}{e_3 b_2}+\frac{b_1^2 e_1}{b_2^2 e_2}\right]^{-1}=\frac{D_m}{D_0} \tag{16}$$

Figure 2 shows the calculations based on Eqs. (15) and (16) using the σ/e_3 values from Fig. 1 for $e_1=1$ by assuming that $e_2=1$ for the uniform as well as the elliptic load distribution since its value for the former is dependent on the actual plan form. The data in Fig. 1 are for $L_1(y_1)$ elliptic and $L_2(y_2)$ either elliptic (solid line for $e_3=1$) or constant (dotted line with $e_3>1$) for gap to larger span ratios of either 0.2 or zero. The calculations for zero gap are shown only for $b_2/b_1>1$, and they were obtained by substituting the σ/e_3 values from Eq. (6) for a constant $L_2(y_2)$ into Eqs. (15) and (16). For $b_2/b_1<1$ the zero gap or coplanar configuration gives $L_1/W=0$ and $D_m/D_0=1$ as long as $e_1=1=e_2$ since the downwash is constant over the rear surface and $\sigma/e_3=\sigma=b_2/b_1<1$ for any $L_2(y_2)$ distribution. It is very important to note that with zero gap D_m/D_0 has a minimum value for $b_1/b_2=0.866$ when the larger rear span has a uniform loading. This minimum value is given directly by Eqs. (6) and (16) which yield the following ratios for the minimum total induced drag when $e_1=1=e_2$

$$\sigma=b_1/b_2=\sqrt{3}/2; \qquad e_3=3/2;$$

$$(D_m/D_0)_{\min}=8/9; \qquad L_1/W=1/3=1/2(L_2/W) \tag{17}$$

for $L_1(y_1)$ elliptic and $L_2(y_2)$ constant.

If $L_2(y_2)$ were also elliptic then we would have $e_1=e_2=e_3=1$ so Eq. (16) would reduce to $D_m/D_0=1$ and $L_1=0$ when the gap is zero so $\sigma=b_1/b_2$. Consequently, D_m is 12.5% greater with an elliptic distribution than it is with a constant load distribution on the 15.5% larger rear span. However, this is a consequence of the assumption that $e_2=1$ even though the rear surface has a constant load distribution rather than the ideal elliptic distribution. For example, if we solve Eq. (16) for the value of e_2 that makes $D_m/D_0=1$, the same as it would be with an elliptic distribution, we find that $e_2=3/4$. Then with $e_3=3/2$ and $\sigma=b_1/b_2=\sqrt{3}/2$, Eq. (15) predicts that this minimum total induced drag is attained when $L_1=W/2=L_2$ for the constant load distribution on the larger span b_2, whereas $L_1=0$ and $L_2=W$ for minimum induced drag when the larger rear span has an elliptic load distribution.

This decrease in the mutually induced drag by the increase in e_3, as given by Eqs. (6) and (9) and shown in Fig. 1, is a result of carrying a greater portion of the lift distribution toward the tips of the larger span wing. When the smaller front span b_1 has an elliptic load distribution, then the outboard portion ($y_2>b_1/2$) of the larger rear span b_2 actually develops an induced "wing thrust" due to the strong upwash given by Eq. (4), also see Ref. 3, p. 151. On the other hand when the larger span becomes the front lifting surface b_1 then its Trefftz-plane downwash over the smaller rear span is decreased as shown by Eq. (8). For example, Eqs. (10) and (11) show that in the limiting case of a very small span rear surface the value of σ is greatly decreased by the uniform load distribution (e.g., σ/e_3 is only one-half that of the elliptic load distribution when the gap is zero).

When the larger rear span has an elliptic distribution then its lift at its outboard sections decreases so rapidly that the "wing thrust" cannot decrease σ/e_3. However, the constant chord rectangular planform lifting surface has a load distribution that carries considerably more of its lift at the outboard sections (e.g., see Ref. 3, p. 184). Numerical calculations based on the data given in Ref. 3 (pp. 177-184) give the following results from Eqs. (2, 4, 15, and 16) for a coplanar small front span ($b_1=0.866\,b_2$) having an elliptic load distribution, when the larger rear span with the constant chord has an aspect ratio of 2π.

$$b_1/b_2=0.866; \qquad e_1=1; \qquad A_2=6.28;$$

$$e_2=0.953; \qquad e_3=1.15;$$

$$L_1/W=0.279; \qquad D_m/D_0=1.01 \tag{18}$$

This configuration would give a distinct advantage for a tandem aircraft since an elliptic load distribution on the larger span rear surface would require that $L_1=0$ for the minimum total induced drag when $e_1=e_2=1=e_3$, and $D_m/D_0=1$, as predicted by Eqs. (15) and (16) for any $\sigma=b_1/b_2<1$.

Since the minimum induced drag can only be attained with zero lift on the smaller span whenever the larger span is coplanar and has an elliptic spanwise load distribution; any canard or tandem aircraft should have a finite gap which is

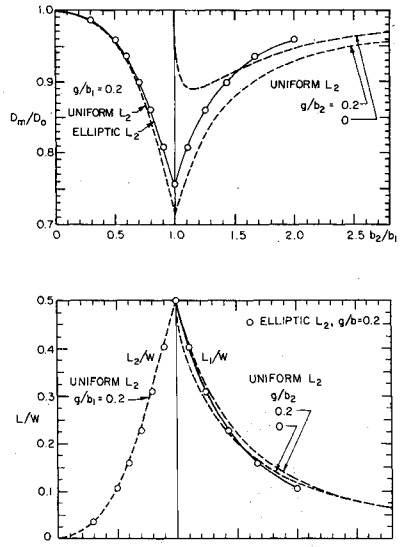

Fig. 2 Minimum induced drag D_m/D_0 and the lift required on the smaller span to attain it. L_1 always elliptic but L_2 either elliptic (solid line) or uniform (dotted line), both calculated with $e_2=1$ so the actual $e_2<1$ for L_2 uniform would raise the dotted lines for D_m/D_0 above the solid lines for L_2 elliptic. Symbols (o) indicate values obtained from the numerical solution of Eqs. (3) and (5) when L_1 and L_2 are elliptic and the gap is one-fifth the larger span.

sufficiently large so that the smaller span can carry its share of the aircraft's weight at the minimum drag condition. For example, Fig. 2 shows that when the gap is one-fifth the larger span, then either an elliptic or a uniform spanwise load distribution on the larger span requires approximately the same lift load on the smaller span in order to attain the minimum induced drag condition.

As shown in Refs. 2 and 4, the usual wing-tail combination has such a relatively small tail span that the induced drag with zero tail load is approximately the same as the minimum induced drag attained with the required small lift load on the tail, for the typical nonzero gap ratios in current use.

References

[1] Prandtl, L., "Induced Drag of Multiplanes," NACA TN 182, March 1924.

[2] Laitone, E.V., "Positive Tail Loads for Minimum Induced Drag of Subsonic Aircraft," *Journal of Aircraft*, Vol. 15, Dec. 1978, pp. 837-842.

[3] Durand, W.F., *Aerodynamic Theory*, Vol. 2, J. Springer, Berlin, 1934, pp. 131-133, 146-151, 177-184, and 216-222.

[4] Laitone, E.V., "Ideal Tail Load for Minimum Aircraft Drag," *Journal of Aircraft*, Vol. 15, March 1978, pp. 190-192.

[5] Sachs, G., "Minimum Trimmed Drag and Optimum C.G. Position," *Journal of Aircraft*, Vol. 15, Aug. 1978, pp. 456-459.